DGAT1 inhibits retinol-dependent regulatory T cell formation and mediates autoimmune encephalomyelitis

Kareem L. Graham[a,1,2], Bonnie J. Werner[a,3], Kimberly M. Moyer[a], Alycia K. Patton[a], Charles R. Krois[b], Hong Sik Yoo[b], Maria Tverskoy[c,4], Melissa LaJevic[d], Joseph L. Napoli[b], Raymond A. Sobel[c], Brian A. Zabel[d], and Eugene C. Butcher[c,1]

[a]Department of Physiology, Emory University School of Medicine, Atlanta, GA 30322; [b]Graduate Program in Metabolic Biology, Department of Nutritional Sciences and Toxicology, University of California, Berkeley, CA 94720; [c]Department of Pathology, Stanford University School of Medicine, Stanford, CA 94305; and [d]Palo Alto Veterans Institute for Research, Veterans Affairs Palo Alto Health Care System, Palo Alto, CA 94304

Edited by Lawrence Steinman, Stanford University School of Medicine, Stanford, CA, and approved December 26, 2018 (received for review October 16, 2018)

The balance of effector versus regulatory T cells (Tregs) controls inflammation in numerous settings, including multiple sclerosis (MS). Here we show that memory phenotype CD4$^+$ T cells infiltrating the central nervous system during experimental autoimmune encephalomyelitis (EAE), a widely studied animal model of MS, expressed high levels of mRNA for *Dgat1* encoding diacylglycerol-O-acyltransferase-1 (DGAT1), an enzyme that catalyzes triglyceride synthesis and retinyl ester formation. DGAT1 inhibition or deficiency attenuated EAE, with associated enhanced Treg frequency; and encephalitogenic, DGAT1$^{-/-}$ in vitro-polarized Th17 cells were poor inducers of EAE in adoptive recipients. DGAT1 acyltransferase activity sequesters retinol in ester form, preventing synthesis of retinoic acid, a cofactor for Treg generation. In cultures with T cell-depleted lymphoid tissues, retinol enhanced Treg induction from DGAT1$^{-/-}$ but not from WT T cells. The WT Treg induction defect was reversed by DGAT1 inhibition. These results demonstrate that DGAT1 suppresses retinol-dependent Treg formation and suggest its potential as a therapeutic target for autoimmune inflammation.

multiple sclerosis | experimental autoimmune encephalomyelitis | neuroinflammation | T regulatory cell | immunometabolism

Multiple sclerosis (MS) is a chronic inflammatory disease of the central nervous system (CNS) that afflicts over 2 million people worldwide. The development of MS is driven by CD4$^+$ T cells that migrate across the blood–brain barrier and into the CNS parenchyma. There is, however, considerable phenotypic and functional heterogeneity among pathogenic CD4$^+$ T cell populations in MS patients (1). The molecular underpinnings of this heterogeneity are complex and incompletely understood, but it is well established that microenvironmental localization and effector functions are tightly linked with CD4$^+$ T cell differentiation status. For example, memory phenotype CD4$^+$ T cells (memCD4Ts), unlike naive T cells, can efficiently enter nonlymphoid tissues and sites of inflammation (2). Myelin antigen-specific memCD4Ts can also achieve full activation in the absence of costimulatory signals, making this lymphocyte subset a potential key contributor to MS pathogenesis and, therefore, a promising target for therapeutic manipulation (3, 4).

To identify mediators of autoimmune CNS inflammation, we performed whole-genome expression analysis of memCD4Ts isolated from tissues of mice with experimental autoimmune encephalomyelitis (EAE) induced by active immunization with myelin oligodendrocyte glycoprotein (MOG) peptide amino acids 35–55 ($MOG_{35–55}$). We found that CNS-infiltrating memCD4Ts from mice with acute clinical EAE expressed high levels of mRNA for diacylglycerol O-acyltransferase-1 (DGAT1), an enzyme that esterifies diacylglycerol in the final step of triglyceride (TG) synthesis (5), and that has been shown to have an important role in esterification of retinol and the regulation of local retinoic acid levels in the skin (6). DGAT1 is expressed at the protein level by adipocytes and macrophages (7), but little is known about DGAT1 function in T cells specifically or in the immune system in general.

Results

Memory CD4$^+$ T Cell Transcriptional Profiling Identifies Key Effector Molecules in EAE. Tissue injury in EAE and MS is driven by pathogenic T cell activation within the CNS, but the microenvironmental cues that influence T cell function and differentiation within the CNS are poorly understood. We reasoned that comparing the expression profiles of CNS vs. lymph node (LN) memCD4Ts would provide insights into novel local microenvironmental regulatory factors and mechanisms that govern effector T cell behavior. We therefore performed transcriptional profiling of FACS-sorted memCD4Ts (CD44^{hi}CD45RB^{lo}CD25$^-$) from CNS and draining LN (dLN) tissues (i.e., inguinal LN) of

Significance

Multiple sclerosis (MS) is a demyelinating disease of the CNS. Experimental autoimmune encephalomyelitis (EAE) is an animal model that has many similarities to MS. CNS-infiltrating, myelin-reactive T cells have pivotal roles in EAE/MS pathology, but the mechanisms governing pathogenic T cell function within the CNS remain poorly understood. Diacylglycerol O-acyltransferase-1 (DGAT1) is a normal lipid- and retinoid-metabolizing enzyme, but little is known about its role in T cells. We show that EAE is reduced in DGAT1-deficient mice. Moreover, our data suggest that T cell expression of DGAT1, by sequestering retinol, limits regulatory T cell (Treg) formation. Overall, our results implicate DGAT1 as a metabolic modulator of Treg induction, and add to the growing appreciation of the interplay between immunity and metabolism.

Author contributions: K.L.G., C.R.K., J.L.N., and E.C.B. designed research; K.L.G., B.J.W., K.M.M., A.K.P., C.R.K., H.S.Y., M.T., M.L., R.A.S., and B.A.Z. performed research; K.L.G., C.R.K., H.S.Y., J.L.N., R.A.S., B.A.Z., and E.C.B. analyzed data; and K.L.G. and E.C.B. wrote the paper.

The authors declare no conflict of interest.

This article is a PNAS Direct Submission.

Data deposition: The microarray data reported in this paper have been deposited in the Gene Expression Omnibus (GEO) database, https://www.ncbi.nlm.nih.gov/geo (accession no. GSE80978).

[1]To whom correspondence may be addressed. Email: kareemlgraham@gmail.com or ebutcher@stanford.edu.

[2]Present address: Second Genome Inc., South San Francisco, CA 94080.

[3]Present address: Division of Scientific Resources, Centers for Disease Control and Prevention, Atlanta, GA 30329.

[4]Present address: Biomarker Operations Program, Genentech, South San Francisco, CA 94080.

This article contains supporting information online at www.pnas.org/lookup/suppl/doi:10.1073/pnas.1817669116/-/DCSupplemental.

Published online February 4, 2019.

mice with acute clinical EAE [13–17 d postimmunization with $MOG_{35–55}$ emulsified in complete Freund's adjuvant (CFA)]. Naive ($CD44^{lo}CD45RB^{hi}CD25^{-}$) and memCD4Ts from peripheral LNs (PLNs) of naive, healthy mice were analyzed for comparison. Sorted populations were >98% pure, as determined by flow cytometry (*SI Appendix*, Fig. S1).

Compared with memCD4Ts from EAE dLN (or memCD4Ts from PLN of naive mice), CNS memCD4Ts had much higher expression of several EAE- and MS-associated genes, such as IFN-γ (*Ifng*) and Fas ligand (*Fasl*). CNS memCD4Ts had relatively lower expression of other key molecules. Examples included: *Cd27*, a costimulatory molecule that represses expression of IL-17A and CCR6 (8); and the trafficking receptors *Ccr7* and L-selectin (*Sell*), consistent with reports that T cells down-regulate these receptors upon entry into extralymphoid tissues (9). CNS memCD4Ts also had up-regulated genes for several transcription factors associated with pathogenic T cell activity, including nuclear receptor subfamily 4, group A, member 2 (*Nr4a2*), which promotes proinflammatory cytokine production by T cells during EAE and MS (10, 11); and cAMP responsive element modulator (*Crem*), which has been linked with autoreactive T helper 17 (Th17) cell differentiation (12). Collectively, the gene signatures were consistent with published real-time reverse-transcriptase quantitative PCR (RT-qPCR) mRNA expression and transcriptome studies of effector T cells in EAE (8, 11, 13), suggesting that a memCD4T-focused profiling approach might identify previously unknown regulators of EAE and MS pathology (Figs. 1 and 2*A* and *SI Appendix*, Table S1).

CNS-Infiltrating Memory Phenotype $CD4^+$ T Cells Express *Dgat1*. The gene for *Dgat1* was highly and selectively expressed by CNS memCD4Ts (Fig. 2 and *SI Appendix*, Table S1). The selectivity of *Dgat1* expression by EAE CNS memCD4Ts, as indicated by the fold-difference in expression compared with that of dLN memCD4Ts, exceeded that of several well-characterized T cell-expressed modulators of EAE and MS pathology, such as *Tnf* and *Stat3* (*SI Appendix*, Table S1). The mean raw expression value of the *Dgat1* gene in CNS memCD4T cells was 8,746, consistent with robust expression. DGAT1 and DGAT2 both catalyze the final step in TG synthesis (14), but *Dgat2* was not significantly up-regulated by CNS memCD4Ts, an observation that we confirmed by RT-qPCR analysis (Fig. 2 *B* and *C*). A query of public microarray datasets (e.g., the Immunological Genome Project and BioGPS) also reveals that, consistent with our microarray and RT-qPCR results, naive and memCD4Ts from peripheral lymphoid tissues do not contain a significant *Dgat1* message; and that *Dgat1* is not expressed in normal brain tissues or cells (e.g., FACS-sorted microglia). Thus, high-level expression of *Dgat1* transcripts by sorted CNS memCD4Ts is likely not caused by contamination from other cell types. Transcripts for lecithin:retinol acyltransferase (*Lrat*), another enzyme with activity that overlaps with DGAT1, also were not detectable in naive or memory phenotype T cells (Fig. 2*B*).

Pharmacologic DGAT1 Inhibition Ameliorates EAE. The up-regulation of *Dgat1* by CNS-infiltrating $CD4^+$ T cells in mice with EAE suggested that DGAT1 might play a role in regulating T cell functions during neuroimmune responses. To address this possibility, we first determined whether pharmacological inhibition of DGAT1 could modulate clinical EAE. Mice induced to develop EAE were administered A922500, a selective DGAT1 inhibitor [molecular mass = 428 Da; IC_{50}: 24 nM for mouse DGAT1 (15)], beginning just before the onset of clinical signs (day 12 postimmunization). Daily administration of 10 mg/kg A922500—which significantly reduces serum TG levels in rodent models of obesity (15)—significantly attenuated clinical EAE. Suppression of clinical disease was

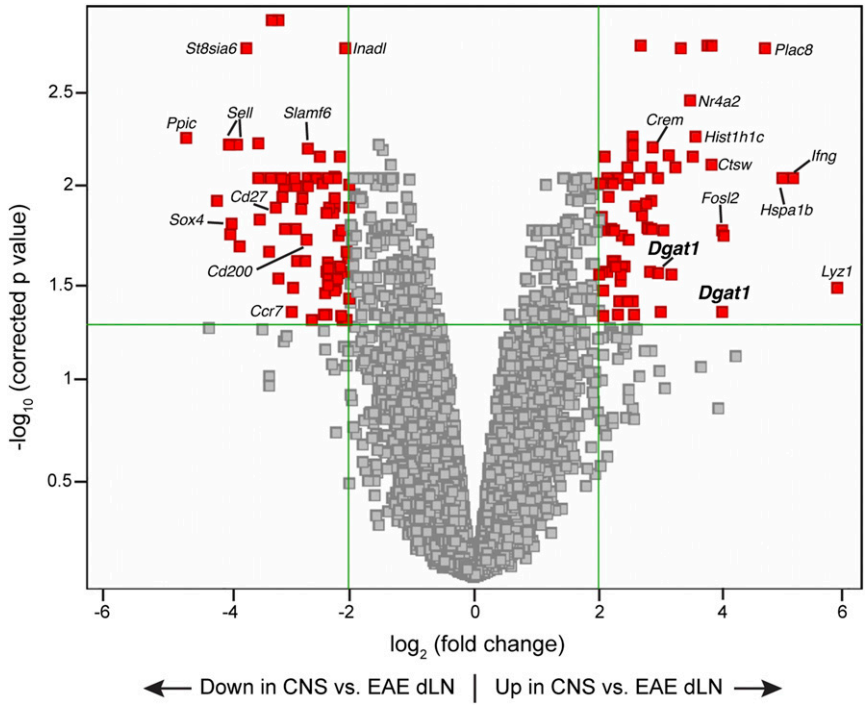

Fig. 1. Transcriptomic analysis of CNS-infiltrating memory $CD4^+$ T cells during EAE. Transcripts in FACS-sorted memCD4Ts derived from female mice with EAE were analyzed using Affymetrix gene chips. GeneSpring software was used for data analysis and visualization (15,288 probes met the selection criteria described in *Methods*). Highly differentially expressed transcripts within CNS memCD4Ts (compared with EAE dLN memCD4Ts) are displayed in volcano plot form. Each symbol represents an individual gene; red symbols indicate transcripts that exhibited at least a fourfold difference in expression value between CNS and EAE dLN memCD4Ts. The complete list of differentially expressed genes can be found in *SI Appendix*, Table S1.

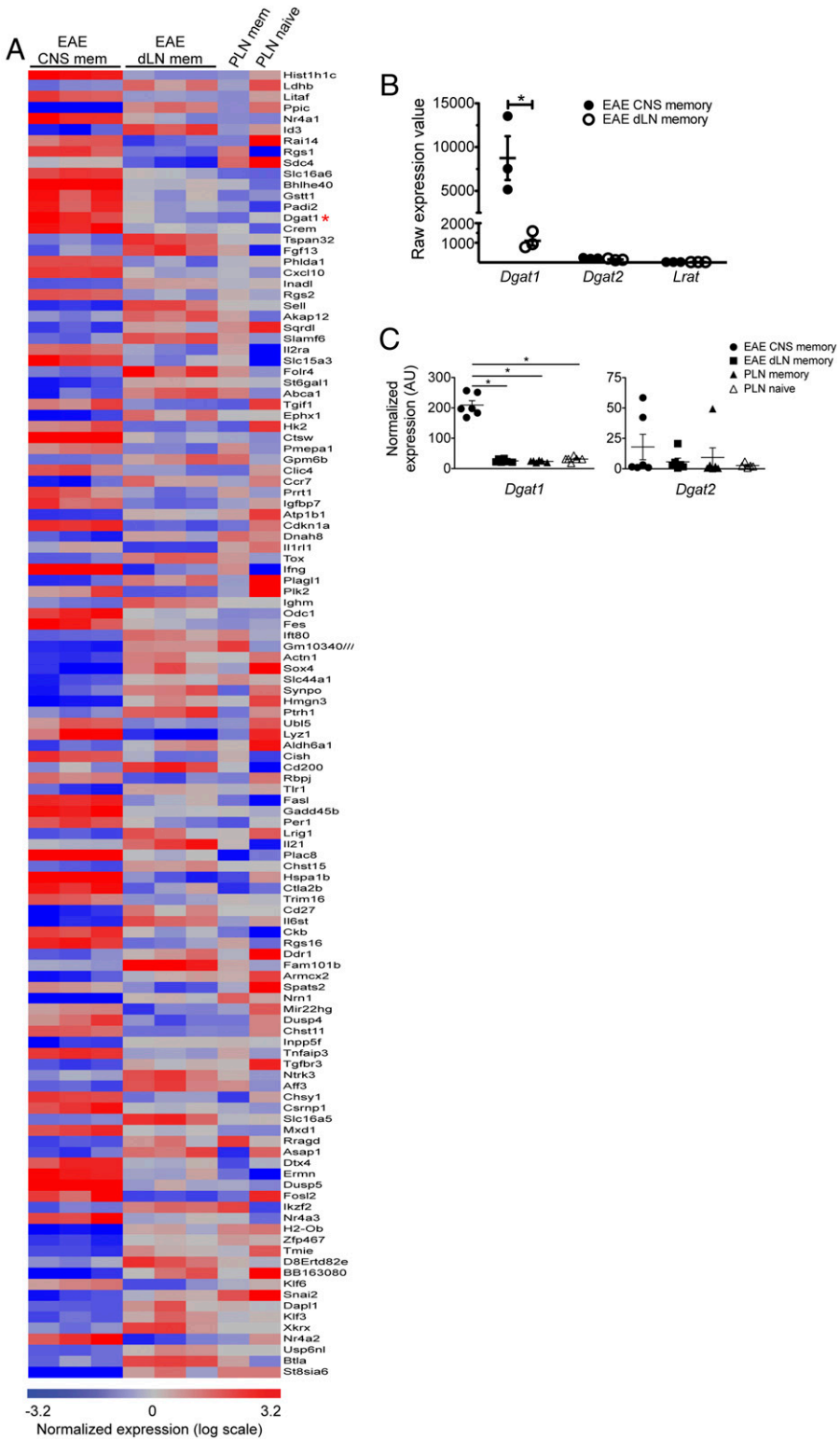

Fig. 2. CNS-infiltrating memory phenotype CD4$^+$ T cells up-regulate Dgat1. Differentially expressed genes identified in Fig. 1 were selected for further analysis. (*A*) Heat map display of genes with at least a fourfold difference in expression in CNS memCD4T versus EAE dLN memCD4T. Each row represents an individual gene, and each column represents an individual experiment/tissue. Red indicates up-regulated genes, while down-regulated genes are in blue. The red asterisk highlights the position of *Dgat1*. (*B*) Scatter plots illustrate low to undetectable raw expression values (as determined by microarray) for *Dgat1*, *Dgat2*, and *Lrat* in EAE dLN, compared with *Dgat1* in CNS memCD4T. Each symbol represents an individual experiment, and the bars depict mean raw expression value ± SEM. *$P < 0.05$ by two-tailed, unpaired Student's *t* test. (*C*) Scatterplots depict RT-qPCR analysis of *Dgat1* (*Left*) and *Dgat2* (*Right*) mRNA expression (normalized to β-actin levels) by naive and memory phenotype CD4$^+$ T cells. Each point represents a biological replicate, and the bars represent mean ± SEM. *$P < 0.05$ by one-way ANOVA with Tukey's multiple comparison test. AU, arbitrary units.

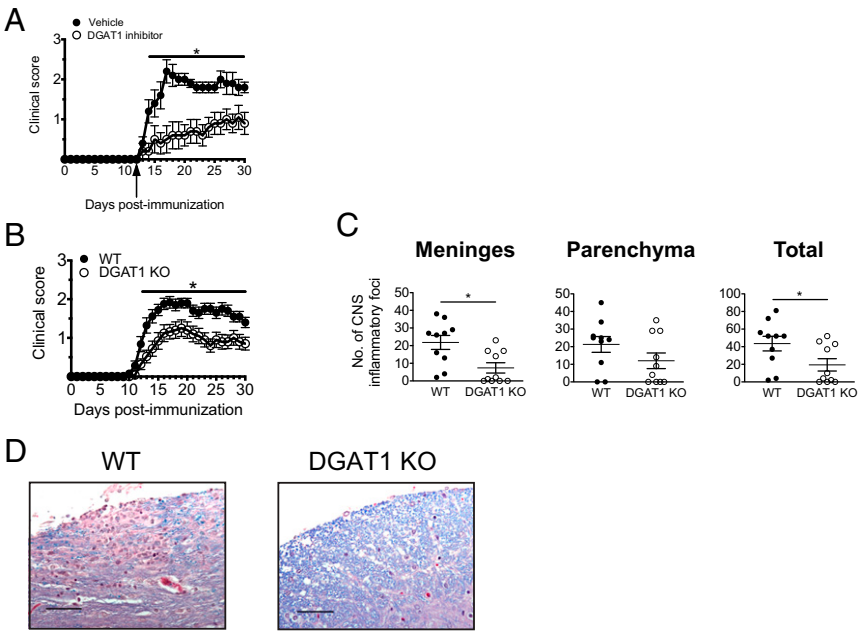

Fig. 3. DGAT1 pharmacologic inhibition and genetic deficiency modulate EAE. (*A*) Female C57BL/6 mice were induced to develop EAE by active immunization with $MOG_{35–55}$/CFA, and then followed daily for clinical signs. Beginning at day 12 postimmunization (arrow), mice were administered vehicle or 10 mg/kg DGAT1 inhibitor via subcutaneous injection once daily (n = 10 mice per group). Clinical data are presented as mean score ± SEM. *P < 0.05 (days 14–30 postimmunization) by Mann–Whitney U test. (*B*) Male C57BL/6 WT and DGAT1 KO mice were induced to develop EAE by active immunization with $MOG_{35–55}$/CFA (n = 25 per group for days 0–17 postimmunization; n = 20 per group for days 18–30 postimmunization). *P < 0.05 for day 12–30 postimmunization, by Mann–Whitney U test. (*C*) Histological changes in meninges and parenchyma at day 30 postimmunization were evaluated as described in *Methods* (total = meninges + parenchyma). Bars represent mean ± SEM. *P < 0.05 by two-tailed, unpaired Student's t test. (*D*) Representative spinal cord sections are shown from WT or DGAT1 KO (mice) actively immunized with $MOG_{35–55}$/CFA and killed at day 30 postimmunization. Meningeal and parenchymal mononuclear cell infiltrates in the spinal cord of a WT mouse (*Left*). Less parenchymal infiltration and reduced demyelination in the spinal cord of a DGAT1 KO mouse (*Right*). Magnification, 40×. (Scale bars, 50 μm.)

evident as early as 2 d after dosing began and persisted until termination of the experiment at day 30 postimmunization (Fig. 3*A*). Overall, the compound delayed onset of clinical signs by an average of 6 d and reduced disease incidence at day 30 postimmunization by 30%. Mice treated with DGAT1 inhibitor also had fewer CNS inflammatory cell infiltrates than their vehicle-treated counterparts, although these differences did not achieve statistical significance (Table 1). Thus, administration of a selective DGAT1 inhibitor attenuates EAE.

DGAT1 Deficiency Attenuates EAE. We next evaluated DGAT1 knockout (KO) mice for susceptibility to EAE. DGAT1 KO mice display resistance to diet-induced obesity and increased energy expenditure (16), but little is known about immune system function in these mice. The frequency of lymphocyte subsets (NK cells, $CD4^+$ T cells, $CD8^+$ T cells, B cells) was similar in WT and DGAT1 KO mouse blood, spleen, and PLN (*SI Appendix*, Fig. S2*A*), suggesting that DGAT1 deficiency does not lead to overt defects in immune cell development. DGAT1 KO mice did, however, have larger LNs and greater numbers of cells overall (*SI Appendix*, Fig. S2*B*).

We found that, when actively immunized with $MOG_{35–55}$/CFA, DGAT1 KO mice developed less severe clinical EAE than their WT counterparts (Fig. 3*B*). To define potential roles for DGAT1 in leukocyte accumulation within or migration to the CNS, we evaluated neural tissues from mice with symptomatic EAE for inflammatory cell infiltrates. Consistent with the clinical findings, CNS tissues isolated from DGAT1 KO mice at day 30 postimmunization contained significantly fewer inflammatory foci and exhibited less demyelination than WT controls (Fig. 3 *C* and *D*).

Role of DGAT1 in EAE Induced by Adoptive Transfer. To determine whether DGAT1 could regulate the induction of EAE by encephalitogenic lymphocytes, we utilized a passive transfer model of disease. We injected naive WT mice with MOG-reactive DGAT1 KO or WT lymphocytes, which were differentiated in vitro under Th17-polarization conditions (17). DGAT1 deficiency in transferred

Table 1. Clinical and pathological EAE in mice treated with a DGAT1 inhibitor

Treatment	Disease incidence	Mean maximal score (SEM)	Mean day of onset (SEM)[†]	No. of CNS inflammatory foci	
				Meninges	Parenchyma
Vehicle	10/10 (100%)	2.5 (0.2)	14.2 (0.4)	41.2 (7.0)	57.0 (9.6)
A922500	7/10 (70%)	1.4 (0.4)[ns]	20.1 (1.9)*	19.8 (8.8)	29.9 (12.4)

Brain and spinal cord tissue was harvested from mice treated with DGAT1 inhibitor A922500 or 10% Captisol vehicle 30 d after induction of EAE by active immunization. Histological changes were evaluated as described in *Methods*; data are presented as mean (SEM). ns, not significant by Mann–Whitney U test (P = 0.05). *P < 0.01 by two-tailed, unpaired Student's t test.

[†]Determined only for animals that developed EAE.

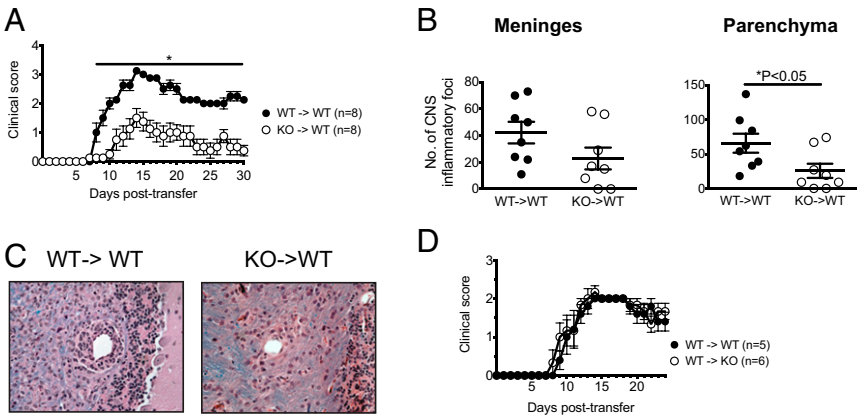

Fig. 4. DGAT1 in encephalitogenic lymphocytes promotes induction of EAE after adoptive transfer. (*A*) Naive male C57BL/6 WT mice were injected with in vitro-generated $MOG_{35–55}$-reactive WT (WT→WT) or DGAT1 KO (KO→WT) lymphocytes. Mice were followed for clinical signs. Data are pooled from two independent experiments (n = 3–5 recipient mice per group for each experiment), and are presented as mean clinical score ± SEM. *$P < 0.05$ by Mann–Whitney U test. (*B*) Histological changes in CNS tissues isolated at 30 d posttransfer from mice that received encephalitogenic lymphocytes were evaluated as described in *Methods*. *$P < 0.05$ by two-tailed, unpaired Student's t test. (*C*) Representative spinal cord sections are shown from WT mice that were injected with in vitro-generated $MOG_{35–55}$-reactive WT (WT→WT) or DGAT1 KO (KO→WT) lymphocytes and killed at 30 d posttransfer. Meningeal and parenchymal mononuclear cell infiltrates typical of acute EAE in the spinal cord of a WT→WT mouse (*Left*). Less parenchymal infiltration in the spinal cord of a KO→WT mouse (*Right*). Magnification, 40×. (*D*) $MOG_{35–55}$-reactive WT lymphocytes were injected into naive male C57BL/6 WT (WT→WT) or DGAT1 KO recipients (WT→KO). Data are pooled from two independent experiments (n = 2–3 recipient mice per group for each experiment), and are presented as mean clinical score ± SEM.

Th17 effector cells had a pronounced effect on the induction of disease. In mice that received polarized DGAT1 KO lymphocytes, EAE onset was delayed by 2.5 d, and the severity of clinical disease was significantly reduced (from day 8 posttransfer onwards) compared with mice that were injected with WT effectors (Fig. 4*A*). Mice that received DGAT1 KO effector cells also had significantly fewer inflammatory foci—and generally exhibited less demyelination—within the CNS parenchyma than mice that received WT effectors at 30 d posttransfer, suggesting that DGAT1 regulates effector cell trafficking to and activation within the CNS (Fig. 4 *B* and *C*). Conversely, WT encephalitogenic Th17 cells induced EAE with similar efficiency upon transfer into WT versus DGAT1 KO hosts (Fig. 4*D*). These results indicate that DGAT1 acts at least in part intrinsically in lymphocytes—presumably via Th17-polarized encephalitogenic lymphocytes—to regulate the development of autoimmune encephalomyelitis.

Effect of DGAT1 Deficiency on IFN-γ^+ or IL-17^+ $CD4^+$ T Cell Induction. To define potential mechanisms for the reduced EAE in DGAT1 KO mice, we evaluated lymphocyte distribution and localization, as well as lymphocyte effector responses. WT and DGAT1 KO CNS tissues from mice with EAE contained statistically indistinguishable percentages and numbers of NK cells, B cells, and $CD4^+$ T cells at day 17 postimmunization (*SI Appendix*, Fig. S3).

We also evaluated $MOG_{35–55}$-recall cytokine-producing T cell frequency in tissues from WT and DGAT1 KO mice with acute EAE (day 17 postimmunization). CNS and dLN cells were restimulated ex vivo with $MOG_{35–55}$, and IL-17^+ and IFN-γ^+ cell frequency was assessed by intracellular cytokine staining. There was no significant difference between WT and DGAT1 KO CNS tissues with respect to absolute numbers or relative frequency of IL-17^+ or IFN-γ^+ $CD4^+$ T cells; and there was a slight but statistically insignificant trend toward increased numbers and percentages of IFN-γ–producing and IL-17–producing $CD4^+$ T cells in DGAT1 KO vs. WT LNs as well. These trends were similar irrespective of whether we analyzed T cell cytokine responses after restimulation with $MOG_{35–55}$ for 72 h; or upon immediate ex vivo stimulation with phorbol 12-myristate 13-acetate (PMA)/ionomycin (Fig. 5 and *SI Appendix*, Fig. S4 *A* and *B*). We also evaluated effector cytokine secretion by leukocytes derived from WT and DGAT1 KO mice with clinical EAE. Upon ex vivo restimulation with $MOG_{35–55}$ peptide for 72 h, CNS mononuclear cells (MNCs) from WT mice with EAE produced proinflammatory cytokines (e.g., IFNγ, IL-17, IL-6, TNF) at levels that trended higher than their DGAT1 KO counterparts. Similarly, DGAT1 KO dLN $CD4^+$ T cells restimulated with $MOG_{35–55}$ in the presence of WT antigen presenting cells capably produced IFN-γ and IL-17; however IFN-γ and IL-17 levels trended higher in cultures with WT dLN $CD4^+$ T cells (*SI Appendix*, Fig. S5). Collectively, our data indicate that DGAT1 KO lymphocytes do not have intrinsic defects in their capacity for Th1 or Th17 cell induction in vivo during EAE.

Regulatory T Cell Distribution in DGAT1 KO Tissues. Regulatory T cells (Tregs) are key modulators of immunopathology in EAE (18). We therefore evaluated WT and DGAT1 KO $CD4^+$ T cells in tissues from mice with EAE for expression of the Treg lineage marker Foxp3 and for CD25. We found that dLNs and CNS tissues from DGAT1 KO mice with EAE contained a significantly higher percentage of $CD25^+Foxp3^+$ Tregs than their WT counterparts (Fig. 6 *A* and *B*). In addition, spleens and PLNs from naive DGAT1 KO mice contained a higher proportion of Tregs than WT controls (*SI Appendix*, Fig. S6), suggesting that DGAT1 may limit Treg development and expansion during both homeostasis and immunity. Collectively, the higher relative proportion of Tregs in DGAT1 KO tissues is consistent with the attenuated clinical EAE exhibited by DGAT1 KO mice.

Evaluating Effects of T Cell-DGAT1 on Treg Formation in Vivo. $DGAT1^{-/-}$ lymphocytes are weak inducers of adoptive EAE (Fig. 4*A*), but both donor and host T cell activation drive clinical EAE in adoptive transfer studies (19). To determine whether T cell-expressed DGAT1 could influence Treg formation in vivo, we performed passive EAE experiments, using B6.CD45.1 congenic mice as recipients of encephalitogenic WT (CD45.2) or $DGAT1^{-/-}$ (CD45.2) lymphocytes. Thirteen days after cell transfer (when mice displayed strong symptomatic EAE), we harvested CNS tissues from recipient mice, and then evaluated $CD25^+Foxp3^+$ Treg frequency within the host (CD45.1) $CD4^+$ T cell compartment by flow cytometry. We found that host-derived $CD4^+$ T cells isolated from mice that received $DGAT1^{-/-}$ lymphocytes contained a higher

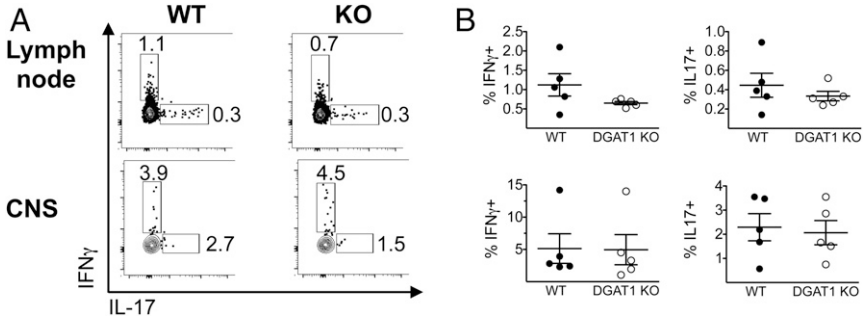

Fig. 5. Effect of DGAT1 deficiency on numbers of IFN-γ– or IL-17–producing CD4$^+$ T cells in dLN and CNS. Male WT and DGAT1 KO mice ($n = 5$ per group) were induced to develop EAE. At day 17 postimmunization, mice were killed. dLN cells (*Upper*) or CNS mononuclear cells (*Lower*) were restimulated for 3 d with $MOG_{35–55}$, and PMA/ionomycin and protein transport inhibitor were added for the last 5 h of the culture period. Cells were then stained with mAbs to surface markers and intracellular cytokines and analyzed by flow cytometry. Viable lymphocytes were gated as NK1.1$^-$CD4$^+$ and evaluated for IFN-γ and IL-17 expression. (*A*) Representative FACS plots indicate the percentage of CD4$^+$ T cells that stained positive for IFN-γ or IL-17 in WT and DGAT1 KO dLNs and CNS. (*B*) Scatter plots indicate the percentage of IFN-γ$^+$ (*Left*) and IL-17$^+$ (*Right*) CD4$^+$ T cells in WT and DGAT1 KO tissues. Each symbol represents an individual mouse; the bar depicts the mean ± SEM. None of the differences achieved statistical significance.

proportion of Tregs than mice that received WT lymphocytes (Fig. 6*C*). Thus, we conclude that T cell-expressed DGAT1 can potentially limit Treg formation *in trans*.

T Cell-Expressed DGAT1 Limits Retinol-Dependent Treg Induction in Vitro. DGAT1 possesses acyltransferase activity toward a number of substrates, including retinol (20). This acyl-CoA:retinol acyltransferase (ARAT) function enables DGAT1 to convert retinol (vitamin A) to its storage retinyl ester form. Retinoic acid (RA), the active metabolite of vitamin A, supports Treg induction (21); however, T lymphocytes cannot synthesize RA autonomously. We hypothesized that T cell expression of DGAT1, by sequestering retinol through esterification, would lead to a reduction in levels of RA locally and thus to reduced Treg formation. Conversely, DGAT1 deficiency would prevent this sequestration of retinol, leading to elevated RA and greater Treg induction. To test this possibility, we stimulated WT or DGAT1 KO CD4$^+$CD25$^-$ T cells (i.e., "non-Tregs") with anti-CD3/TGF-β in the presence of mesenteric lymph node (MLN) and Peyer's patch (PP) antigen-presenting and stromal cells (dissociated MLN plus PP cells depleted of T cells). Dendritic cells and stromal fibroblastic reticular cells in MLN and PP express high levels of the retinol dehydrogenase and retinal dehydrogenase enzymes necessary for converting retinol to RA (22, 23). We used DGAT1 KO ($^{-/-}$) MLN/PP stromal cells for antigen presentation, to ensure that any potential

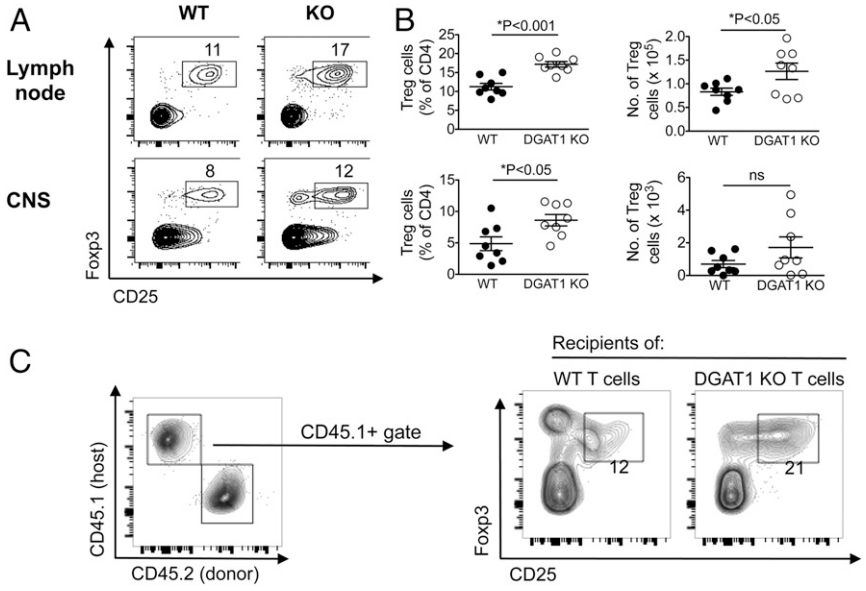

Fig. 6. DGAT1 influences Treg frequency in lymphoid and CNS tissues. Male C57BL/6 and DGAT1 KO mice ($n = 8$ per group) were induced to develop EAE by immunization with $MOG_{35–55}$/CFA. At day 17 postimmunization, mice were killed and cells in dLN or CNS tissues were analyzed by flow cytometry. NK1.1$^-$CD4$^+$ lymphocytes were then analyzed for expression of CD25 and Foxp3. (*A*) Representative FACS plots indicate the frequency of CD25$^+$Foxp3$^+$ Tregs in dLN and CNS tissues of WT and DGAT1 KO mice. Numbers represent the percentage of Tregs within the gate. (*B*) Scatter plots indicate the percentage (*Left*) or number (*Right*) of CD4$^+$ Tregs in WT and DGAT1 KO tissues. Each symbol represents an individual mouse; the bar depicts the mean ± SEM. *$P < 0.0001$ or $P < 0.05$ by two-tailed, unpaired Mann–Whitney *U* test (*Left*); or *$P < 0.05$ by two-tailed, unpaired Student's *t* test (*Right*). ns, not significant. (*C*) Naive male B6/CD45.1 WT mice were injected with in vitro-generated $MOG_{35–55}$-reactive WT (CD45.2) or DGAT1 KO (CD45.2) CD4$^+$ T cells. Thirteen days later, CNS MNCs were harvested and pooled from recipient mice ($n = 4$ per group). Viable CD4$^+$ lymphocytes were gated on the CD45.1 (host) allotype, and then evaluated for expression of CD25 and Foxp3 by flow cytometry. Two independent experiments with similar results were performed.

DGAT1-dependent effects on retinol responses were mediated by the T cell compartment.

We found that in vitro anti-CD3/TGF-β stimulation induced Tregs with similar efficiency from WT and DGAT1 KO naive ($CD25^-$) T cell precursors. Addition of low levels of retinol (10 nM) to the culture significantly enhanced $Foxp3^+$ Treg induction from $DGAT1^{-/-}$, but not from WT ($DGAT1^{+/+}$) $CD4^+$ $CD25^-$ T cells, consistent with an inhibitory role for DGAT1 in RA generation and signaling. Addition of the DGAT1 inhibitor A922500—as well as higher levels of retinol (100 nM)—abrogated the difference between $DGAT1^{-/-}$ and WT $CD4^+$ T cell responses. Moreover, DGAT1 deficiency had no significant effect on enhanced Treg induction by the synthetic RA receptor agonist AM580 (Fig. 7 and *SI Appendix*, Fig. S7). Notably, DGAT1 did not significantly impact in vitro differentiation of naive $CD4^+$ T cell precursors into Th1 or Th17 effectors, as determined by frequency of IFN-γ^+ or IL-17^+ cells, respectively. Additionally, retinol supplementation inhibited WT and DGAT1 KO IL-17–producing $CD4^+$ T cell generation with similar efficiency (*SI Appendix*, Fig. S8). Collectively, our results show that T cell-expressed DGAT1 limits retinol-dependent Treg formation, but that DGAT1 does not significantly impact Th1 or Th17 differentiation in vitro or in vivo. Quantitative analysis of tissue retinoids reveals that levels of retinyl ester—but not RA or retinol—in DGAT1 KO lymph nodes are significantly lower than their WT counterparts. Compared with their respective naive counterparts, retinyl ester levels were higher in LNs derived from WT and DGAT1 KO mice with EAE; however, the differences achieved statistical significance only when comparing retinyl ester levels in WT EAE vs. WT naive mice. The results indicate a unique and key role within the LN for DGAT1 in converting retinol, a precursor of RA, into its retinyl ester storage form (*SI Appendix*, Fig. S9).

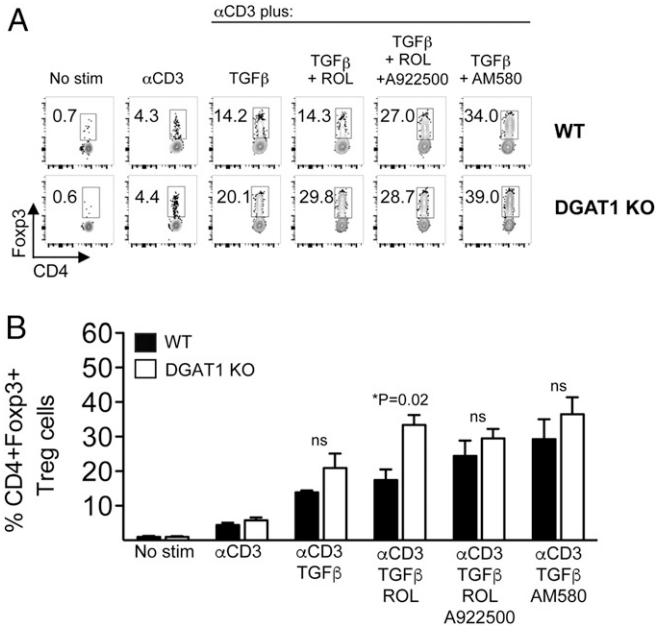

Fig. 7. DGAT1 limits retinol-dependent Treg induction. Female WT or DGAT1 KO $CD4^+CD25^-$ cells were incubated with T cell-depleted DGAT1 KO MLN stromal cells in delipidated serum in the absence or presence of: soluble anti-CD3, TGF-β, retinol (ROL; 10 nM), A922500 (100 nM), or AM580 (10 nM) where indicated. After 3 d, $TCR\beta^+$ lymphocytes in the live gate were analyzed for expression of CD4 and Foxp3 by flow cytometry. (*A*) Representative FACS plots show the frequency of WT (*Upper*) or DGAT1 KO (*Lower*) $CD4^+Foxp3^+$ Tregs within the gate. (*B*) FACS data are summarized in bar graph form. Bars depict the mean + SEM of triplicate wells. Two independent experiments with similar results were performed. *$P = 0.02$ (WT vs. DGAT1 KO) by two-tailed, unpaired Student's *t* test. ns, not significant.

Discussion

Comparative proteomics and transcriptomic studies have the potential to uncover novel regulatory pathways and pathogenic mechanisms in EAE and MS (24–26). The clinical and histological heterogeneity of MS, however, presents challenges for applying "omics" approaches to identify tractable therapeutic targets. Here, we focused our analyses on discrete T lymphocyte subsets within the CNS and lymphoid tissues of mice with EAE. We report that memory phenotype $CD4^+$ T cells isolated from spinal cords of mice with acute clinical EAE express high levels of mRNA for *Dgat1*. Parenteral administration of a pharmacologic DGAT1 inhibitor, as well as genetic DGAT1 deficiency, attenuated EAE; and healthy mice that received encephalitogenic, in vitro-polarized DGAT1 KO Th17 cells exhibited delayed EAE onset, reduced disease, and increased Treg frequency (compared with mice that received WT Th17 cells), suggesting a cell-intrinsic role for T cell-expressed DGAT1 in EAE pathology. In addition, CNS and lymphoid tissues from DGAT1 KO mice contained a higher proportion of Treg cells, consistent with our observations of more efficient in vitro Treg induction from naive DGAT1 KO $CD4^+$ T cells in the presence of retinol. DGAT1 is closely related to a second diacylglycerol acyltransferase, DGAT2. Both enzymes catalyze the final and essential step in TG synthesis, but only DGAT2 is essential in vivo (27). We did not, however, detect significant *Dgat2* message in T cells. Moreover, DGAT2 lacks ARAT or other acyltransferase activity (20).

Attenuation of EAE by a selective DGAT1 inhibitor provides a proof-of-concept demonstration that this enzyme may be a viable target for therapy of autoimmune demyelinating disease. Although we began dosing with the inhibitor before the appearance of overt clinical signs (mean day of disease onset in vehicle-treated mice = 14.2, while dosing began at day 12), CNS cellular activation and T lymphocyte infiltration of the CNS precede development of clinical EAE (28–30). While the extent to which the inhibitor crosses the blood–brain barrier has not been experimentally determined, it may not be necessary for the drug to cross the blood–brain barrier for efficacy, as autoreactive T cell polarization and activation likely occurs in PLNs. Nevertheless, the ability of the A922500 inhibitor to ameliorate EAE when administered therapeutically suggests that it has contemporaneous effects on cells within the CNS (both resident and recruited) and influences on inflammatory cell activation within the periphery.

Retinol, the circulating form of vitamin A, is converted to retinal and then to RA by retinol dehydrogenase (RDH) and retinal dehydrogenase (RALDH) enzymes, respectively. The binding of RA to specific retinoic acid receptors in activated T cells has myriad effects on gene transcription and cellular differentiation, including but not limited to induction of Tregs (21). Levels of retinol and RA are therefore tightly regulated in vivo. RA synthesis from circulating retinol via retinaldehyde is controlled not only by cell-specific expression of RALDH enzymes, but also by mechanisms that sequester retinol in retinyl ester form for storage or to suppress local RA synthesis. Recent studies show that DGAT1 is a retinol acyltransferase and that it critically regulates RA synthesis from retinol: in an in vivo model of vitamin A effects on the epidermis, DGAT1 deficiency led to excessive RA and to RA-dependent development of alopecia (6). Our studies support a similar role for T cell DGAT1 in control of physiologic retinol-mediated responses (summarized schematically in *SI Appendix*, Fig. S10): We found that DGAT1 KO but not DGAT1-sufficient (WT) $CD4^+CD25^-$ T cells showed enhanced Treg differentiation in the presence of retinol and stromal cells capable of converting available retinol to RA.

RA has other regulatory effects on T cell activation and function, including inhibition of T effector cell differentiation (31). We observed a trend toward reduced Th1 and Th17 cell numbers in the LNs of immunized DGAT1 KO (vs. WT) mice during EAE, but the differences from WT were not significant. Consistent with this, because T effector cell commitment occurs in LNs before migration to the CNS, Th1 and Th17 frequencies in the CNS were also unaffected. The robust DGAT1-dependence of CNS inflammation in the active EAE model may thus principally reflect DGAT1 suppression of Treg generation or survival. However, roles in other aspects of T effector cell responses are not excluded (see discussion below).

In addition to its role in inhibiting Treg induction during active EAE induction, our results indicate that DGAT1 is required for maximal induction of EAE by adoptively transferred encephalitogenic Th17 cells in immunocompetent hosts. RA is known to inhibit effector cell functions, including IL-17 secretion by committed Th17 cells (31). DGAT1 in CNS T effector cells—by sequestering retinol—may thus support pathogenic cytokine production when retinol, through an RDH/RALDH-expressing cell, would otherwise be a source of RA. Lack of DGAT1 in KO mice, or in adoptively transferred DGAT1$^{-/-}$ Th17 cells, may allow RA synthesis and lead to cytokine suppression. Indeed, the synthetic RA receptor agonist AM580 limits IL-17 secretion during EAE (32). Notably, adoptive transfer of DGAT1$^{-/-}$ Th17 cells is associated with elevated Treg frequency in host CNS tissues, which may be partly due to higher local levels of RA in EAE lesions that are populated by DGAT1$^{-/-}$ vs. WT T cells (Fig. 6*C*). Our results suggest that T cell-expressed DGAT1 can limit Treg formation *in trans*, although we do not exclude the possibility that DGAT1 might also influence T effector cell activity via regulation of RA availability *in cis*. Further investigation of potential roles for DGAT1 in regulating Th17 cell functions is warranted.

The ability of T cell-expressed DGAT1 to regulate retinol and RA-dependent outcomes locally may have broad effects on T cell responses in the CNS. Interestingly, low serum levels of retinol are associated with increased MS risk, and serum retinol levels are inversely correlated with magnetic resonance imaging outcomes in MS (33, 34). However, in addition to regulating retinol and RA, DGAT1 may also impact T cell function through its activity on other substrates. DGAT1 was initially identified as a diacylglycerol acyltransferase capable of mediating the terminal step of TG synthesis. During an immune response, TGs may serve as an energy storage molecule during T cell activation (35). Lipid metabolism pathways can also function as regulators of activated lymphocyte function and differentiation (36, 37).

Classically, LRAT is considered the enzyme most responsible for synthesis of retinyl ester and retinoid storage, and systemically this is clearly the case: ~80% of the body's retinoids are stored in LRAT-dependent lipid droplets within hepatic stellate cells (38). It is surprising therefore, that DGAT1 deficiency is sufficient to nearly eliminate retinyl ester storage in LNs (*SI Appendix*, Fig. S9). The major source of free retinol in the steady state is via uptake from the blood, and consistent with this, retinol levels are similar in WT and DGAT1 KO LNs (*SI Appendix*, Fig. S9). However, current models suggest that physiologically significant RA production is controlled locally at the sites of cell–cell interaction to imprint activated T cells. In these sites, we hypothesize that there may be a competition for retinol, with DGAT1 shunting the precursor to the inactive storage pool, competing with dendritic cells or stromal cell RALDH enzymes that generate RA for juxtacrine signaling. Collectively, our data demonstrate a unique role for DGAT1 in converting retinol to retinyl ester in lymph nodes compared with skin and liver (6, 39). However, our results do not exclude the possibility that other enzymatic activities of DGAT1 underlie the observed moderation of Treg induction in the WT setting.

In this study, we focused on roles for DGAT1 in Th17 cell-mediated pathology and effector functions, but we do not exclude effects on other immune cells. For example, neutrophils, which express significant levels of *Dgat1* message (Immunological Genome Project data), can also contribute to pathology during EAE (40). Additional genetic studies (e.g., evaluation of immune functions in conditional DGAT1 KO mice) will further illuminate roles for DGAT1 in regulating the activity of CD4$^+$ T cells and other leukocyte subsets.

In summary, we demonstrate that memory CD4$^+$ T lymphocytes up-regulate *Dgat1* messages during autoimmune CNS inflammation, and that DGAT1 pharmacologic inhibition and genetic deficiency significantly ameliorate EAE and enhance Tregs within lymphoid and CNS tissues. In addition, T cell-expressed DGAT1 limits retinol-mediated Treg formation in vitro. These results add to the growing appreciation of the interplay between immune and metabolic pathways. They also suggest that DGAT1 inhibitors, which have been evaluated in trials for metabolic diseases, should be assessed for roles in therapy of MS and potentially other disorders associated with Th17 or Treg cell imbalance.

Methods

Mice and Reagents. DGAT1 KO.CD45.2 (B6.129S4-*Dgat1*$^{tm1Farl/J}$), C57BL/6.CD45.2 WT, and C57BL/6.CD45.1 WT (B6.CD45.1) mice were purchased from The Jackson Laboratory and bred in the animal facility at Emory University. DGAT1 WT littermate controls were also generated and bred at Emory University. $MOG_{35–55}$ (MEVGWYRSPFSRVVHLYRNGK) was synthesized by the Stanford Protein and Nucleic Acid Facility. The DGAT1 inhibitor A922500 was purchased from Selleck Chemical Company. Captisol (Cydex Pharmaceuticals), a modified cyclodextrin that has a favorable drug formulation profile (41), was used as the vehicle for A922500 for in vivo dosing studies. Normal FBS was from HyClone, and delipidated FBS was from Gemini Bio-Products. Cell culture media ("complete RPMI") consisted of RPMI 1640 supplemented with 10% FBS (normal or delipidated), penicillin/streptomycin, L-glutamine, minimum nonessential amino acids, sodium pyruvate, 20 mM Hepes buffer, and 50 μM 2-mercaptoethanol. Antibodies directed against T cell receptor-β (TCR-β) (H57-597), NK1.1 (PK136), CD25 (PC61), CD44 (IM7), CD45RB (C363.16A), CD45.2 (104), CD45.1 (A20), Foxp3 (FJK-16s), CD4 (RM4-5), CD8 (53.6–7), CD3ε (145-2C11), IFN-γ (XMG1.2), IL-17A (TC11-18H10), anti–IL-4 (11B11), and anti–IFN-γ (R4-6A2) were from eBioscience or BD Biosciences; and fixable cell viability dye was from eBioscience. FlowJo software (TreeStar) was used for analysis of flow cytometry data. PMA and ionomycin (Sigma) were used at 50 ng/mL and 500 ng/mL, respectively. Protein transport inhibitor (containing monensin and brefeldin A) was from eBioscience. Recombinant mouse IL-6, IL-12, IL-23, and TGF-β were from R&D Systems. All-*trans*-retinol was from Sigma, and AM580 was from Tocris Biosciences. Where indicated, T cell-depleted MLN cells (5×10^6 cells/mL) were incubated with 50 μg/mL mitomycin C (Sigma) for 20 min at 37 °C. Cells were then extensively washed in PBS, followed by coincubation with WT or DGAT1 KO CD25- T cells in U96 plates (37 °C, 5% CO_2).

EAE Models. For EAE induction by active immunization, mice (8- to 10-wk-old) were immunized via subcutaneous injection with 100 μg $MOG_{35–55}$ emulsified in CFA, as described previously (42). Mice also received 250 ng pertussis toxin (List Biological Labs) via tail vein injection at the time of $MOG_{35–55}$/CFA immunization and again 2 d later. Clinical disease was scored as follows: 0 = normal or healthy; 1 = flaccid tail; 2 = hindlimb weakness; 3 = hindlimb paralysis; 4 = hindlimb and forelimb paralysis; 5 = moribund or dead. Male mice were used in all experiments except where indicated. For pharmacologic inhibition studies, the DGAT1 inhibitor A922500 was formulated in 10% Captisol vehicle for in vivo dosing via subcutaneous injection (100 μL volume). Individuals who conducted the clinical scoring (K.L.G. or K.M.M.) were blinded to the treatment that the mice received.

For EAE induction by adoptive transfer, WT or DGAT1 KO mice were immunized subcutaneously with $MOG_{35–55}$/CFA. Mice received 250 ng pertussis toxin via intraperitoneal injection at the time of $MOG_{35–55}$/CFA immunization and again 2 d later. Ten days after immunization, spleens and dLN cells (i.e., inguinal LN) were harvested, pooled and resuspended in complete RPMI (with normal FBS) at 5×10^6 cells/mL. Cells were incubated with $MOG_{35–55}$ (10 μg/mL) plus IL-23 (10 ng/mL) to generate Th17-polarized cells. After 72 h in culture (37 °C, 5% CO_2), cells were washed extensively

with PBS, and then resuspended in PBS before intraperitoneal injection into healthy, naive recipients (8- to 10-wk-old 0.5–1 × 10^7 cells per mouse).

Cell Sorting and Microarray Analysis. For transcriptional profiling of T cells from female mice with MOG-induced active EAE, dLN, and spinal cord tissues were harvested and pooled (n = 20–25 mice per experiment, three independent experiments) at the time of peak acute disease (~13–17 d post-immunization). MNCs from spinal cords were isolated over 30%:70% discontinuous Percoll gradients (42). $CD4^+$ T cells from dLN tissues of mice with EAE, as well as from pooled PLNs (axillary, brachial, and inguinal) of naive C57BL/6 mice (8- to 10-wk-old), were isolated by negative selection with magnetic beads (Miltenyi). Memory $CD4^+$ T cells (memCD4T; $CD44^{hi}CD45RB^{lo}CD25^-$) and naive phenotype ($CD44^{lo}CD45RB^{hi}CD25^-$) $CD4^+$ T cells from LNs, as well as memCD4T derived from CNS MNCs, were then sorted on an Aria II instrument. RNA from FACS-sorted cells was isolated with a Qiagen RNeasy Kit, and 100–200 ng total RNA from each sample was used for amplification, labeling, and hybridization on Affymetrix mouse 430 2.0 arrays by the Stanford Protein and Nucleic Acid Facility. Microarray data were analyzed using GeneSpring GX 13.0 software. Gene-expression values were normalized with the RMA16 algorithm of GeneSpring for the visualization and analysis of microarrays. Probes were then filtered by expression value (at least three of the four conditions within the dataset—CNS memCD4T; EAE dLN memCD4T, PLN memCD4T; PLN naive—had to show an average raw value above 120). To enrich for highly differentially expressed genes within CNS-infiltrating T cells, genes in the CNS memCD4T cell subset with expression values that differed by at least fourfold ($P < 0.05$, Benjamini–Hochberg correction) from the EAE dLN memCD4T cell subset were selected for additional analysis. Microarray data were deposited in the Gene Expression Omnibus (GEO) database (GSE80978) (43).

RT-qPCR. Total RNA from memory and naive phenotype $CD4^+$ T cells was isolated by TRIzol extraction, and gene expression was measured by RT-qPCR using a QuantiFast One-Step RT-PCR Kit (Qiagen) according to the manufacturer's instructions. Samples were analyzed using an Applied Biosystems 7900HT real-time PCR instrument. Mouse primer sequences were as follows: β-actin forward, 5′– GTATCCATGAAATAAGTGGTTACAGG–3′; β-actin reverse, 5′–GCAGTACATAATTTACACAGAAGCAAT–3′. DGAT1 forward, 5′–CCCAT-ACCCGGGACAAAGAC–3′; DGAT1 reverse, 5′–ATCAGCATCACCACACACCA–3′. Primers for DGAT2 were used as described previously (7).

T Cell Differentiation and $MOG_{35–55}$ Recall Assays. PLN tissues from C57BL/6 WT or DGAT1 KO mice (8–10 wk) were depleted of $CD4^+CD25^+$ T cells by using a T regulatory cell isolation kit (Miltenyi). MLN tissues and PP from sex-matched DGAT1 KO mice were depleted of T cells via CD90.2 magnetic beads (Miltenyi). To generate Tregs, $CD4^+CD25^-$ cells (10^5) were incubated with T cell-depleted, mitomycin C-treated DGAT1 KO MLN/PP feeder cells (4×10^4) in the presence of TGF-β (5 ng/mL), and soluble anti-CD3 (0.25 μg/mL). For Th1 differentiation, $CD4^+CD25^-$ cells were incubated with DGAT1 KO MLN/PP feeders in the presence of anti-CD3 plus IL-12 (10 ng/mL) and anti–IL-4 (10 μg/mL). For Th17 differentiation, $CD4^+CD25^-$ cells were stimulated with DGAT1 KO feeder cells, anti-CD3, TGF-β (3 ng/mL), IL-6 (20 ng/mL), anti–IL-4 (10 μg/mL), and anti–IFN-γ (10 μg/mL). MLN/PP cells were >99% free of T cells following CD90.2 bead depletion, and PLN cells were >99% $CD4^+CD25^-$ following $CD25^+$ cell depletion, as determined by flow cytometry.

In some experiments, CNS mononuclear cells from mice with symptomatic EAE were stimulated (10^5 cells per well) with a dose-range of $MOG_{35–55}$ peptide. In other experiments, dLN $CD4^+$ T cells were isolated by negative selection with magnetic beads and incubated (5×10^4 per well) with mitomycin C-treated splenocytes (2.5×10^5 per well) in the presence of a dose-range of $MOG_{35–55}$. Cytokine levels in culture supernatants were measured after 72 h using ELISA kits according to the manufacturer's instructions (eBioscience).

Retinoid Quantitation. Retinyl ester, retinol, and RA were extracted from mouse LNs as described previously (44). Quantification of retinoids was done using liquid chromatography-tandem mass spectrometry (LC-MS/MS) with an alternate LC separation.

Histology. Brain and spinal cord tissues were fixed in 10% buffered formalin. Formalin-fixed tissue was embedded in paraffin and sections were stained with Luxol fast blue-H&E stain. CNS inflammatory foci (>10 mononuclear cells per focus) in leptomeninges and parenchyma were counted in each mouse sample in a blinded fashion by one of the authors (R.A.S.).

Statistics. The Mann–Whitney U test was applied to analyze nonparametric clinical EAE data, and the Student's t test was used to analyze all parametric data. The Fisher's exact test was used to compare disease incidence.

Study Approval. All animal experiments and procedures were approved by and conducted in accordance with Emory, US Department of Veterans Affairs, and NIH Institutional Animal Care and Use Committee guidelines.

ACKNOWLEDGMENTS. This project benefited greatly from the use of Immunological Genome Project data. We thank Rocky Bilhartz, Joel Haas, and Robert V. Farese, Jr. for helpful discussions; Ashlee Zheng for technical assistance; and the Emory University School of Medicine Flow Cytometry Core and Lusijah Rott (Stanford University) for assistance with flow cytometry analysis and cell sorting. This work was supported by: Research Scholar Development Award K22 AI81878, a Woodruff Scholar Early Career Independence award from Emory University, and a University Research Committee award from Emory University (to K.L.G.); Grants R01 AI093981, R01 DK084647, and R37 AI047822 (to E.C.B.); the US Department of Veterans Affairs (E.C.B. and B.A.Z.); and in part by Merit Review Award I01 BX004115 from the US Department of Veterans Affairs Biomedical Laboratory R&D Service (to B.A.Z.). M.T. was a recipient of fellowship support under NIH training Grants 5 T32 AI07290 and T32 CA09151.

1. Pierson E, Simmons SB, Castelli L, Goverman JM (2012) Mechanisms regulating regional localization of inflammation during CNS autoimmunity. *Immunol Rev* 248: 205–215.
2. Campbell DJ, Debes GF, Johnston B, Wilson E, Butcher EC (2003) Targeting T cell responses by selective chemokine receptor expression. *Semin Immunol* 15:277–286.
3. Lovett-Racke AE, et al. (1998) Decreased dependence of myelin basic protein-reactive T cells on CD28-mediated costimulation in multiple sclerosis patients. A marker of activated/memory T cells. *J Clin Invest* 101:725–730.
4. Markovic-Plese S, Cortese I, Wandinger KP, McFarland HF, Martin R (2001) CD4+CD28– costimulation-independent T cells in multiple sclerosis. *J Clin Invest* 108:1185–1194.
5. Cases S, et al. (1998) Identification of a gene encoding an acyl CoA:diacylglycerol acyltransferase, a key enzyme in triacylglycerol synthesis. *Proc Natl Acad Sci USA* 95: 13018–13023.
6. Shih MY, et al. (2009) Retinol esterification by DGAT1 is essential for retinoid homeostasis in murine skin. *J Biol Chem* 284:4292–4299.
7. Koliwad SK, et al. (2010) DGAT1-dependent triacylglycerol storage by macrophages protects mice from diet-induced insulin resistance and inflammation. *J Clin Invest* 120: 756–767.
8. Coquet JM, et al. (2013) The CD27 and CD70 costimulatory pathway inhibits effector function of T helper 17 cells and attenuates associated autoimmunity. *Immunity* 38: 53–65.
9. Engelhardt B, Martin-Simonet M-TG, Rott LS, Butcher EC, Michie SA (1998) Adhesion molecule phenotype of T lymphocytes in inflamed CNS. *J Neuroimmunol* 84:92–104.
10. Raveney BJ, Oki S, Yamamura T (2013) Nuclear receptor NR4A2 orchestrates Th17 cell-mediated autoimmune inflammation via IL-21 signalling. *PLoS One* 8:e56595.
11. Doi Y, et al. (2008) Orphan nuclear receptor NR4A2 expressed in T cells from multiple sclerosis mediates production of inflammatory cytokines. *Proc Natl Acad Sci USA* 105: 8381–8386.
12. Koga T, et al. (2014) CaMK4-dependent activation of AKT/mTOR and CREM-α underlies autoimmunity-associated Th17 imbalance. *J Clin Invest* 124:2234–2245.
13. Hoppmann N, et al. (2015) New candidates for CD4 T cell pathogenicity in experimental neuroinflammation and multiple sclerosis. *Brain* 138:902–917.
14. Cases S, et al. (2001) Cloning of DGAT2, a second mammalian diacylglycerol acyltransferase, and related family members. *J Biol Chem* 276:38870–38876.
15. Zhao G, et al. (2008) Validation of diacyl glycerolacyltransferase I as a novel target for the treatment of obesity and dyslipidemia using a potent and selective small molecule inhibitor. *J Med Chem* 51:380–383.
16. Smith SJ, et al. (2000) Obesity resistance and multiple mechanisms of triglyceride synthesis in mice lacking Dgat. *Nat Genet* 25:87–90.
17. Axtell RC, et al. (2010) T helper type 1 and 17 cells determine efficacy of interferon-beta in multiple sclerosis and experimental encephalomyelitis. *Nat Med* 16:406–412.
18. Yu P, et al. (2005) Specific T regulatory cells display broad suppressive functions against experimental allergic encephalomyelitis upon activation with cognate antigen. *J Immunol* 174:6772–6780.
19. Lees JR, Iwakura Y, Russell JH (2008) Host T cells are the main producers of IL-17 within the central nervous system during initiation of experimental autoimmune encephalomyelitis induced by adoptive transfer of Th1 cell lines. *J Immunol* 180: 8066–8072.
20. Yen CLE, Monetti M, Burri BJ, Farese RV, Jr (2005) The triacylglycerol synthesis enzyme DGAT1 also catalyzes the synthesis of diacylglycerols, waxes, and retinyl esters. *J Lipid Res* 46:1502–1511.
21. Mucida D, et al. (2007) Reciprocal TH17 and regulatory T cell differentiation mediated by retinoic acid. *Science* 317:256–260.
22. Iwata M, et al. (2004) Retinoic acid imprints gut-homing specificity on T cells. *Immunity* 21:527–538.

23. Hammerschmidt SI, et al. (2008) Stromal mesenteric lymph node cells are essential for the generation of gut-homing T cells in vivo. *J Exp Med* 205:2483–2490.
24. Han MH, et al. (2008) Proteomic analysis of active multiple sclerosis lesions reveals therapeutic targets. *Nature* 451:1076–1081.
25. Han MH, et al. (2012) Janus-like opposing roles of CD47 in autoimmune brain inflammation in humans and mice. *J Exp Med* 209:1325–1334.
26. Garris CS, et al. (2013) Defective sphingosine 1-phosphate receptor 1 (S1P1) phosphorylation exacerbates TH17-mediated autoimmune neuroinflammation. *Nat Immunol* 14:1166–1172.
27. Stone SJ, et al. (2004) Lipopenia and skin barrier abnormalities in DGAT2-deficient mice. *J Biol Chem* 279:11767–11776.
28. Luo J, et al. (2007) Glia-dependent TGF-β signaling, acting independently of the TH17 pathway, is critical for initiation of murine autoimmune encephalomyelitis. *J Clin Invest* 117:3306–3315.
29. Murphy AC, Lalor SJ, Lynch MA, Mills KH (2010) Infiltration of Th1 and Th17 cells and activation of microglia in the CNS during the course of experimental autoimmune encephalomyelitis. *Brain Behav Immun* 24:641–651.
30. Sobel RA, Blanchette BW, Bhan AK, Colvin RB (1984) The immunopathology of experimental allergic encephalomyelitis. II. Endothelial cell Ia increases prior to inflammatory cell infiltration. *J Immunol* 132:2402–2407.
31. Xiao S, et al. (2008) Retinoic acid increases Foxp3+ regulatory T cells and inhibits development of Th17 cells by enhancing TGF-beta-driven Smad3 signaling and inhibiting IL-6 and IL-23 receptor expression. *J Immunol* 181:2277–2284.
32. Klemann C, et al. (2009) Synthetic retinoid AM80 inhibits Th17 cells and ameliorates experimental autoimmune encephalomyelitis. *Am J Pathol* 174:2234–2245.
33. Salzer J, et al. (2013) Vitamin A and systemic inflammation as protective factors in multiple sclerosis. *Mult Scler* 19:1046–1051.
34. Loken-Amsrud KI, et al. (2013) Retinol levels are associated with magnetic resonance imaging outcomes in multiple sclerosis. *Mult Scler* 19:451–457.
35. Yen CL, Stone SJ, Koliwad S, Harris C, Farese RV, Jr (2008) Thematic review series: Glycerolipids. DGAT enzymes and triacylglycerol biosynthesis. *J Lipid Res* 49:2283–2301.
36. Bensinger SJ, et al. (2008) LXR signaling couples sterol metabolism to proliferation in the acquired immune response. *Cell* 134:97–111.
37. Michalek RD, et al. (2011) Cutting edge: Distinct glycolytic and lipid oxidative metabolic programs are essential for effector and regulatory CD4+ T cell subsets. *J Immunol* 186:3299–3303.
38. Blaner WS, et al. (2009) Hepatic stellate cell lipid droplets: A specialized lipid droplet for retinoid storage. *Biochim Biophys Acta* 1791:467–473.
39. Ajat M, et al. (2017) Hepatic stellate cells retain the capacity to synthesize retinyl esters and to store neutral lipids in small lipid droplets in the absence of LRAT. *Biochim Biophys Acta Mol Cell Biol Lipids* 1862:176–187.
40. Steinbach K, Piedavent M, Bauer S, Neumann JT, Friese MA (2013) Neutrophils amplify autoimmune central nervous system infiltrates by maturing local APCs. *J Immunol* 191: 4531–4539.
41. Cruz-Orengo L, et al. (2011) CXCR7 antagonism prevents axonal injury during experimental autoimmune encephalomyelitis as revealed by in vivo axial diffusivity. *J Neuroinflammation* 8:170.
42. Graham KL, et al. (2009) Chemokine-like receptor-1 expression by central nervous system-infiltrating leukocytes and involvement in a model of autoimmune demyelinating disease. *J Immunol* 183:6717–6723.
43. Graham KL (2016) DGAT1 regulates retinol-dependent regulatory T cell generation and mediates autoimmune encephalomyelitis. Gene Expression Omnibus. Available at https://www.ncbi.nlm.nih.gov/geo/query/acc.cgi?acc=GSE80978. Deposited May 2, 2016.
44. Bhattacharya N, et al. (2016) Normalizing microbiota-induced retinoic acid deficiency stimulates protective CD8(+) T cell-mediated immunity in colorectal cancer. *Immunity* 45:641–655.